Active Load Management of Hydrogen Refuelling Stations for Increasing the Grid Integration of Renewable Generation

IEEE Access
Multidisciplinary | Rapid Review | Open Access Journal

Date of publication xxxx 00, 0000, date of current version xxxx 00, 0000.

Digital Object Identifier 10.1109/ACCESS.2017.Doi Number

Active Load Management of Hydrogen Refuelling Stations for Increasing the Grid Integration of Renewable Generation

Wei Sun (Member, IEEE), AND Gareth P. Harrison (Senior Member, IEEE)

School of Engineering, The University of Edinburgh, Edinburgh EH9 3FB, U.K.

Corresponding author: Wei Sun (w.sun@ed.ac.uk)

The work has been funded by EPSRC, UK, through the 'Hydrogen's Value in the Energy System (HYVE)' project (grant number EP/L018284/1) and the EPSRC National Centre for Energy Systems Integration (grant number EP/P001173/1).

ABSTRACT Hydrogen Fuel Cell Electric Vehicles (FCEV) can help reduce carbon emissions, air pollution and dependency on fossil fuels in the transport sector. Clean hydrogen fuel can be generated by a power-to-gas process at refuelling stations equipped with water electrolysers, especially in renewable rich areas. Coupled with onsite hydrogen tanks, the fast response capability of electrolysis, could potentially turn the station demand into a flexible electricity load since the hydrogen can be stored and used when needed. This paper presents a novel real-time load management scheme that actively operates a hydrogen refuelling station to relieve thermal network constraints, handles the fluctuations from renewables, and releases network headroom for connecting renewable generation. The key components involved in the refuelling station and their operational characteristics are explicitly modelled in the analysis. The economic impact of the different operational strategies is also examined. In the case study, the effectiveness of the proposed control strategy to avoid overloading and save curtailment in the local distribution network is verified by running the real-time network simulation at 1 minute steps over a 1 hour window and 5 day window respectively. Moreover, a whole year simulation of the station operation shows that the proposed active control strategy enables wind farms in the local network to avoid 9.5 times more curtailment than under passive control strategy. The station's net cost of electricity consumption thus can be reduced by 7.5%., by making use of excess electricity that would otherwise be curtailed. A further 5% reduction on the cost would be possible if the incentive rewards for offering network constraint management services are in place.

INDEX TERMS Power-to-gas, hydrogen vehicle, flexible demands, active network management, renewable energy, multi-energy integration

I. INTRODUCTION

Transport represents a major source of greenhouse gas emissions and is the main cause of air pollution in cities [1], [2]. The use of fossil-fuelled internal combustion engines that still dominate the transport sector needs to be drastically reduced [3] and hydrogen (H_2) could be an important part of the answer to the emission reduction challenge in the transport sector. Hydrogen as a transportation fuel can be produced from renewable energy sources and its use in fuel cell electric vehicles (FCEV) is an effective approach to reduce carbon emissions, air pollution and dependency on fossil fuels [4]. However, the shift towards hydrogen-fuelled vehicles depends on the clean production of hydrogen and the widespread availability of hydrogen refuelling stations.

The performance of hydrogen fuelled FCEV has significantly improved in the recent years. There are various models commercially available from major automobile manufacturers, such as Honda, Hyundai, Nissan and Fiat. Recent years have seen a large number of hydrogen-fuelled vehicle projects being implemented around the world. The roll-out of hydrogen-fuelled vehicles in the UK is ongoing, including various types of passenger cars, buses and heavy-goods vehicles, accompanied by the development of refuelling stations [5]. The UK has two of the largest stations in Europe, with plans to expand the number of stations in the coming years [6].

While some advocate hydrogen networks based around large central generation using steam methane reformation [7], on-site hydrogen production at refuelling stations through grid

This article has been accepted for publication in a future issue of this journal, but has not been fully edited. Content may change prior to final publication. Citation information: DOI 10.1109/ACCESS.2021.3098161, IEEE Access

connected electrolysis is also a promising option as it can avoid the cost and safety concern of shipping hydrogen via pipeline or truck [8]. This could be generated from electricity in the local electricity network and is especially attractive where this is from renewable generation either onsite or in the vicinity. There are several trials in the UK looking at this [9], [10].

In distribution networks that already operate near thermal (i.e. power flow) capacity, the additional electricity consumption from hydrogen refuelling stations would be challenging to accommodate. Exploring the flexibility of on-site electrolysers to handle the fluctuations from renewables would be a potential solution in these cases. Distribution networks in renewable rich areas, such as Scotland, are struggling to accommodate more wind or PV installations without (major) network reinforcement at distribution and transmission level. The constraints in these networks are due to electricity export from local generation rather than import. Deploying hydrogen refuelling stations in these areas and controlling their power demand to manage constraints could provide additional headroom to connect new renewable generation. In addition, the use of on-site hydrogen storage tanks, which feature longer time-duration and greater storage quantities [11], allows refuelling station electricity load to be decoupled from its hydrogen fuel demand for a considerable period. The value of supporting renewable integration from hydrogen refuelling stations would therefore be further enhanced. Thus, the integration of hydrogen refuelling stations into the electricity network to meet transport demand, has the potential to be coordinated with the rapid development of renewable generation for clean hydrogen production. The modelling and control of such interlinked local systems among electricity, hydrogen and transport is essential for decision making and pre-feasibility analysis.

Operation and control of hydrogen refuelling stations has been studied from several different aspects, typically categorised by whether analysis considers connection to the electricity network or operation as part of an islanded microgrid. Without explicitly considering where the electricity came from, [12] looked at minimising the overall energy consumption while [13] minimised refuelling time. In the context of renewable integration, the studies on hydrogen refuelling stations further split into those at aggregate national level [14], [15], or detailed studies of individual stations accommodated in local distribution networks. For example, [16] used an optimal power flow method to consider half-hourly power management of electrolysers and storage of hydrogen to maximise wind generation in a constrained distribution network. [17] looked at the cost optimal operation of a refuelling station with onsite wind turbine subject to market prices and a constrained substation.

Active control for electricity network constraint management, in general, remains an active research area and a wide range of centralised and decentralized approaches have also been proposed. The fluctuations of renewable production, demand and potentially FCEV refuelling require advanced control schemes to operate on relatively short time scales (seconds to minutes) in order to manage power flow and voltage constraints without damage from sustained overloads or non-compliance with voltage regulations. The use of active control can maximize use of the existing assets, release extra headroom for new demand and more renewable distributed generation (DG). Zhou and Bialek [18] present a generation curtailment approach for multiple DG units to manage voltage constraints. Sansawatt et al. [19] propose a decentralized control strategy to mitigate voltage rise and line overloads; it uses a real-time sensitivity method with reactive power control and generation curtailment to manage constraints local to the DG connection. Robertson et al. [20] employ sophisticated optimal power flow-based real-time scheduling of network controls and DG settings to better integrate high levels of DG, in a coordinated and synchronised manner. A centralized control algorithm is developed and trialled in [21], which uses limited information to manage EV charging points to mitigate simultaneous thermal and voltage problems in LV networks. No study except the authors' recent conference paper [22] appears to consider hydrogen refuelling stations as part of the active network management scheme in real-time distribution network operation. This paper substantially extends the work [22] in terms of scope and depth of modelling methodology, analysis and case studies (e.g. full station model and new economic impact evaluation, etc.).

The work presented here proposes operational control strategies for hydrogen refuelling stations such that management of the station electrical load can be used to solve network thermal constraints. To illustrate the value of the operational control of refuelling stations, the paper employs an active network control framework based on the sensitivity method to calculate the ongoing operating point of the refuelling station. However, the approach could be used within other active control methods. While several existing studies have demonstrated that the wide adoptions of distributed electrolysis could make significant contributions to integrate intermittent renewables from the global, national and large regional view [23]–[25], the research on the real-time control of the electrolysis in a refueling station to rapidly and effectively manage network constraints caused by the continuous variation of nearby renewable generation at short time scales is still sparse. The contribution of the work is the use of a hydrogen refuelling station to establish a novel, active and real-time network control scheme, specifically in medium-voltage distribution network, which can help manage the rapid variation of local renewable generation and avoid curtailment. The modelling used in this study is important in investigating the technical feasibility and economic performance of active control of refuelling stations in providing flexibility to handle fluctuations from renewables. While there are undoubtedly similarities in the challenges and potential benefits of battery EVs and hydrogen refuelling stations, there are a range of specific technical characteristics

This article has been accepted for publication in a future issue of this journal, but has not been fully edited. Content may change prior to final publication. Citation information: DOI 10.1109/ACCESS.2021.3098161, IEEE Access

which warrant analysis. In particular the specific components involved in the refuelling station and their operational characteristics are explicitly captured.

The paper is structured as follows: Section II describes modelling of a hydrogen refuelling station and its electricity load. The design of different control strategies is described in Section III, including an evaluation approach for understanding their economic performance. In Section IV, the validation of the proposed strategy through a case study is presented. The remainder discusses and concludes the work.

II. MODELLING OF GRID-CONNECTED HYDROGEN REFUELLING STATION

The hydrogen refuelling station considered in this study aims to meet the demand of FCEV cars. It consists of electrolysers which use electricity supply from the grid connection to split water into hydrogen; compressors which raise the gas pressure ready for storage tanks and dispensing and fuel dispensers with cooling systems which enable filling of the FCEVs. Figure 1 shows a schematic of the station. The whole process of converting electricity to compressed hydrogen is subject to energy losses. The modelling of each component and its energy demand is described below, using equivalent energy on the same basis where possible, to avoid confusion between energy and mass of hydrogen.

A time series basis modelling approach is used that is able to operate on a range of time steps (minutes to hours). It describes the flow of energy over multiple time steps, accounting for the various stages of the process and changes in on site storage. The decisions about how much hydrogen is produced, and specifically the power demand is taken as part of the operating strategy of the refuelling station, as described in Section III.

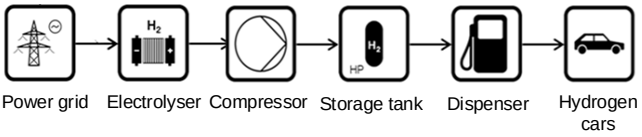

FIGURE 1. Generic model of the hydrogen refuelling station with power-to-gas production and grid connection [26]

A. ELECTROLYSER

Electrolysers produce hydrogen via the electrolysis of water using electricity. It is environmentally-friendly when using electricity sourced from renewable energy and produces high purity hydrogen that is favoured by fuel cell vehicles [27]. Different types of electrolysers are available mainly due to the different type of electrolyte material involved [28]. They vary in terms of simplicity, efficiency, and production capacity. Among them, Proton Exchange Membrane electrolysers (PEMs) [29] and alkaline electrolysers [30] are popular.

The electrical power consumption (MW) at the inlet of the electrolyser ($P_{in,elser,t}$) in time period t is given by:

$$P_{in,elser,t} = P_{out,elser,t}/\eta_{elser} \quad (1)$$

where $P_{out,elser,t}$ (MW) is the equivalent power that is contained in the hydrogen produced at the electrolyser outlet. η_{elser} is the conversion efficiency of the electrolyser. A PEM electrolyser is considered in this paper and the electrolyser efficiency is treated as a constant across its operating range (with a typical range 60-80% [29]). This is a first level approximation and is reasonable when considering small changes in operating point of the electrolyser. More sophisticated efficiency characteristics could be used.

While electrolysers can be operated above their rated power levels, for simplicity, the power consumption of the electrolyser is limited by its rated power P^{+}_{elser} and minimum allowed input P^{-}_{elser} (MW):

$$P^{-}_{elser} \leq P_{in,elser,t} \leq P^{+}_{elser} \quad (2)$$

The ability to increase and decrease the electrolyser power consumption between successive time periods $t-1$ and t is limited to:

$$\sigma^{-}_{elser} \leq \frac{P_{in,elser,t} - P_{in,elser,t-1}}{\tau_t} \leq \sigma^{+}_{elser} \quad (3)$$

where σ^{+}_{elser} and σ^{-}_{elser} are the maximum ramp up/down rates (MW/time) and τ_t is the duration of period t (h).

The mass flow rate of hydrogen produced by the electrolyser (kg/h) is given by:

$$m_{elser,t} = \frac{P_{out,elser.t}}{HHV_{h2}} \quad (4)$$

where HHV_{h2} is the higher heating value of hydrogen (39.4 kWh/kg).

B. COMPRESSOR

Hydrogen produced by commercial electrolysers can be at pressures of 10 to 50 bar, while the pressure required to fill hydrogen FCEVs is 350 bar or 700 bar [31]. Therefore, compressors are required to raise the pressure from the outlet of the electrolyser to these higher pressures. The electricity consumption (W_{comp}, MW) of the compressor is determined by [32]:

$$W_{comp,t} = \lambda_{comp} \cdot m_{comp,t} \quad (5)$$

where m_{comp} is the flow rate of H_2 gas (kg/h) and the λ_{comp} is given by:

$$\lambda_{comp} = C_p \frac{T_1}{3600\,\eta_{comp}} \left(\left(\frac{\pi_2}{\pi_1} \right)^{\frac{r-1}{r}} - 1 \right) \quad (6)$$

where C_p is the specific heat of hydrogen at constant pressure (14.304 kJ/kg K); T_1 is the compressor's inlet gas temperature (assumed to be a constant 293 K); η_{comp} is the efficiency of the compressor; π_1 and π_2 are the inlet and output pressures (bar); and r is the isentropic exponent of hydrogen (1.4). In practice, compressors have complex operational characteristics and limitations as conditions vary. However, for simplicity, the

This article has been accepted for publication in a future issue of this journal, but has not been fully edited. Content may change prior to final publication. Citation information: DOI 10.1109/ACCESS.2021.3098161, IEEE Access

compressor efficiency was set at 0.8 across the full range of operation with the compression ratio and λ_{comp} both considered as constants.

The compressor mass flow rate is limited by its rated maximum flow rate, m_{comp}^{rated}:

$$m_{comp,t} \leq m_{comp}^{rated} \tag{7}$$

For the system as show in Figure 1, unless operating beyond its rating, the flow rate of the compressor matches that of the outlet of electrolyser:

$$m_{comp,t} = m_{elser,t} \tag{8}$$

C. STORAGE

A high-pressure storage tank is used to store the high pressure hydrogen coming from the outlet of the compressor and is then connected to the fuel dispensers. Beside the provision of buffering and reserve capacity, hydrogen storage has the potential to enable flexible changing of the station electricity consumption to respond to network constraints, for example, during periods with excess renewable generation. The control scheme discussed in section III will investigate the value of this in detail.

As before, the storage of hydrogen is considered in energy terms, with the amount of hydrogen in storage at any point in time constrained as follows:

$$E_{stor}^{-} \leq SOC_{stor,t} \leq E_{stor}^{rated} \tag{9}$$

where $SOC_{stor,t}$ is the amount of energy equivalent hydrogen stored within the storage tank at the time t; E_{stor}^{rated} is the rated storage capacity and E_{stor}^{-} is the minimum storage value to be maintained at all times (all MWh).

For simplicity, the round-trip efficiency of storage is considered with its input flow as:

$$SOC_{stor,t} = SOC_{stor,t-1} + m_{comp,t} \cdot \eta_{stor} \cdot \tau_t \cdot HHV_{h2} - H_{2\,dem,t} \cdot \tau_t \cdot HHV_{h2} \tag{10}$$

where $m_{comp,t}$ is the rate of hydrogen flowing into storage from the compressor; η_{stor} is round-trip efficiency; and $H_{2\,dem,t}$ (kg/h) is hydrogen dispensed to fill vehicles matching that flowing out of storage. The storage of hydrogen is reasonably efficient with limited leakage over time.

D. STATION ELECTRICITY LOAD MODEL

There are other components in the refuelling station, such as dispensers to transfer hydrogen from storage tanks to the on-board tanks of the hydrogen FCEVs. A pre-cooling system is necessary in order to cool hydrogen down to a safe temperature to counter isenthalpic expansion during the filling process. Their energy consumption is however relatively small [33] and neglected here.

It is assumed that at any given moment, the electrolyser and compressor will operate together to deliver hydrogen into the storage tank, but that the outflow from storage through the dispenser will be independent of this. If the electrolyser and compressor are sized accordingly, the flow rate is the same for the electrolyser outlet, compressor and storage inlet during operation. Therefore, by accounting for energy losses and electricity consumed during the whole process of converting electricity to dispensed hydrogen as presented in Eq. (1)-(10), the overall efficiency (i.e. energy conversion ratio) of the refuelling station can be derived as:

$$\eta_{stn} = \frac{\eta_{elser}\,\eta_{stor}\,HHV_{h2}}{\eta_{elser}\lambda_{comp} + HHV_{h2}} \tag{11}$$

III. OPERATING STRATEGIES FOR H_2 REFUELLING STATIONS

The main operating purpose of the refuelling station is to serve the demand from FCEVs over a defined horizon period. This aim can be achieved through a relatively simple and straightforward operational strategy, termed here as 'passive mode', in which hydrogen is produced to match demand in a given period. Beyond this fundamental operational target, and with the support of onsite storage, the refuelling station could also be operated in alternative modes, in order to serve additional technical and economic targets. 'Steady' operation involves maintaining a flat hydrogen production profile to allow smaller rated electrolysers and compressors as well as easing wear and tear on the equipment. 'Active' operation combines a scheduled flat hydrogen production profile with adaptive adjustment of electrolysers' scheduled power input in order to provide electricity network support.

All the control strategies were implemented in the OpenDSS distribution network simulator [34], which is capable of quickly solving complex power flows. The OpenDSS simulator is provided with the full information of the distribution network (including the network layout and the characteristics of power lines, transformers) as well as electricity demand, wind output and H_2 refuelling station scheduled demand. It performs the time series simulations of the distribution network as well as implementing the corresponding control of the H_2 refuelling station.

A. PASSIVE OPERATION MODE

The control flow for the 'passive' operating model is outlined in Figure 2. At the beginning of each control period, the hydrogen fuel demand of the period is estimated and converted to equivalent power consumption of the station. Here, the (electrical) power input to the refuelling station ($P_{h2,t}$P$_{h2,t}$) is used to produce only the amount of hydrogen demanded by FCEVs in each period:

$$P_{h2,t} = \frac{H_{2\,dem,t}}{HHV_{h2} \cdot \eta_{stn} \cdot \tau_t} \tag{12}$$

In this passive mode, hydrogen generation aims to match the changing FCEV hydrogen demand within and between each period. The varying characteristics of hydrogen production would require a large electrolyser and compressor to be installed to meet the peak hydrogen demand that may

This article has been accepted for publication in a future issue of this journal, but has not been fully edited. Content may change prior to final publication. Citation information: DOI 10.1109/ACCESS.2021.3098161, IEEE Access

only occur for a few hours or minutes. In addition, the continuously changing profile of production would also cause wear and tear of the equipment and reduce its lifetime. In this operating mode, storage is used to provide backup reserve for any outage in the hydrogen production. While storage also provides a buffer to smooth out the filling if any minor mismatch occurs within period *t*, in this paper only multiple-hours of storage capacity is considered which is used to balance the mismatch between periods.

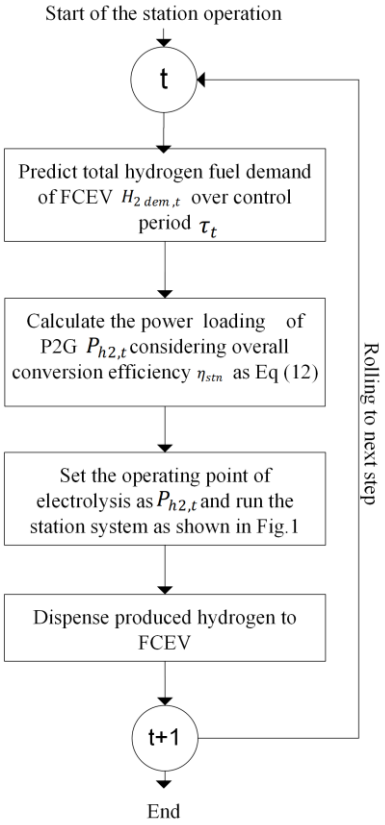

FIGURE 2. Outline of control model for 'passive' operation of the refuelling station

B. STEADY OPERATION MODE (WITH STORAGE SUPPORT)

To serve the same amount of total hydrogen with a day, rather than continuously varying the hydrogen production to follow demand at each time steps (as in the passive mode), operating the refuelling station at a continuous rate has advantages in reducing the required size of the electrolyser and compressor, as well as its wear and tear. A 'steady operation' strategy is proposed to maintain production at a fixed rate throughout the day, with the equivalent electricity demand calculated based on the hourly average of the total hydrogen daily demand:

$$P_{h2,t} = \frac{1}{24}\sum_{t=1}^{T}\frac{H_{2\,dem,t}HHV_{h2}}{\eta_{stn}} \tag{13}$$

The control flow of steady operation is outlined in Figure 3. The main differences from the passive mode are the day-ahead scheduling step which initiates the whole process as well as storage control to offset the mismatch between hydrogen production and demand in specific periods. Figure 3 also contains a dashed box which is the additional step required for the 'active' operation mode that uses the steady operation mode as its basis (see Section III.C).

Owing to the variation in the number of FCEVs served in each period within the day, the mismatch between hydrogen production and actual hydrogen demand will need to be provided by onsite hydrogen storage. The amount of hydrogen in storage $SOC_{h2,t}$ at the end of each period, can be calculated as:

$$SOC_{h2,t} = SOC_{h2,t-1} + P_{h2,t}\cdot\eta_{stn}\cdot\tau_t - H_{2\,dem,t}\cdot HHV_{h2} \tag{14}$$

If the demand is correctly foreseen, at the end of the day the storage will return to the start-of-day level. This mode of operation will result in the correct volume of hydrogen in storage being built up ahead of peak demand periods and reduced afterwards.

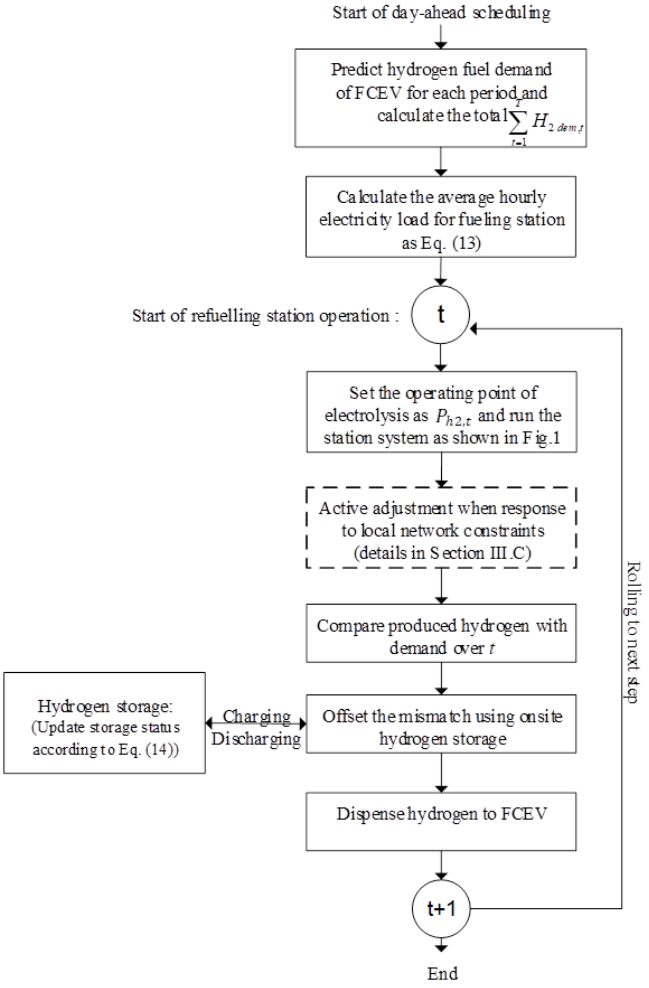

FIGURE 3. Outline of control model for 'steady operation' of the refuelling station (with option for 'active' control highlighted in the dashed box).

This article has been accepted for publication in a future issue of this journal, but has not been fully edited. Content may change prior to final publication. Citation information: DOI 10.1109/ACCESS.2021.3098161, IEEE Access

C. ACTIVE OPERATION MODE WITH NETWORK CONSTRAINT MANAGEMENT

The electrolyser has the capability to rapidly change its operating point within a few seconds [11]. With onsite hydrogen storage tanks to store the unscheduled hydrogen generation, the refuelling station electricity load can be decoupled from its hydrogen demand for a few hours. An 'active' response approach, on top of normal steady operation, is proposed here aiming to provide fast mitigation of network issues, by providing adaptive changes in the refuelling station's electricity load.

It is important to point out that the network overloading event considered here is due to high production from the local DG, leading to export of power towards the higher voltage network. Therefore, increasing refuelling station demand will tend to relieve congestion by consuming more of the DG output locally. This is opposite to the case where overloading is caused by local peak demand, although the principles are similar.

This active control approach is identical to the steady-state mode (Figure 3) but with the extra step indicated by the dashed box. This extra step is the control logic that governs any intervention made to the station operation to mitigate network issues that may have arisen; **Figure 4** shows the control logic which operates on a rolling basis from one time step to the next. The logic is similar to the approach in [19] and requires the loading of the critical network component to be monitored on an ongoing basis with the loading condition communicated to the controller at the refuelling station. The location of the critical network component will be network specific and would be determined through offline analytical studies.

The control scheme employs a persistence forecasting approach wherein the network demand and DG production at time *t* are expected to remain the same for the rest of the period up to *t*+1. At each point in time the power flow on the monitored feeder or transformer is checked to see whether it is above or below a defined threshold level and appropriate actions taken based on this. The threshold is generally considered to be the thermal rating of the network component or some value just below it to minimise the risk that changes in demand or DG production within the period *t* to *t*+1 will create a significant overload. The operation is explained in detail in the following subsections.

1) NORMAL OPERATION

The normal operational state of the refuelling station is based on the scheduled operating points and would be expected to dominate the operation period. In this study, the scheduled load is set as the value that meets the hourly average of the daily hydrogen demand, i.e. the same as the steady operation case calculated by Eq. (13). The refuelling station will operate at the (day ahead) scheduled load value unless (1) a network overload is sensed or (2) there no overload but there is more hydrogen in storage than the scheduled amount at that particular point in time. The control scheme responds to these differently by respectively raising electrical demand at the refuelling station through 'overproduction' of hydrogen, or reducing the stock of stored hydrogen through 'underproduction' and lowering electrical demand; the next subsections deal with these cases in turn.

2) OVERPRODUCTION

If at time step *t*, the power flow $S_{measured,t}$ at the monitored line/transformer exceeds the threshold value $S_{threshold}$, the control system views this as an 'overloading' event. The control system reacts to this in the next time step *t*+1, by instructing that more electricity will be consumed locally by increasing hydrogen production, i.e. 'overproduction' such that the power flow reduces to a new, lower, target level, $S_{targeted}$.

The refuelling station target power input is set to an increased value $P_{h2,t+1}$ as calculated by:

$$P_{h2,t+1} = P_{h2,t} + \Delta P^{+}_{h2,t+1} \tag{15}$$

where $\Delta P^{+}_{h2,t}$ is the increase in station electricity demand required to reach the lower target line/transformer loading level. The controller needs to identify the necessary change in demand $\Delta P^{+}_{h2,t}$ and as the relationship between station demand and component loading is governed by the power flow equations, strictly speaking a nonlinear optimisation would be required to explicitly determine the necessary change in demand to deliver the consequent change in loading level. However, sensitivity analysis offers a fast linear approximation to this with reasonably low error [19], [35].

This uses the derivative of line/transformer loading level with refuelling station demand at the initial operating point to estimate the demand level which delivers the desired loading level:

$$\Delta P^{+}_{h2,t+1} = \frac{S_{measured,t} - S_{targeted}}{\delta S_t \,/\, \delta P_{h2,t}} \tag{16}$$

where the numerator is the required change in component loading from the measured value $S_{measured,t}$ to the target level and the denominator is the sensitivity factor $\delta S_t \,/\, \delta P_{h2,t}$ which estimates how component loading varies with station demand.

There are a number of ways of estimating the sensitivity factor, and the Discussion elaborates on how it can be carried out in practice. Here, it is estimated using two power flow simulations using slightly different network loading conditions. The first power flow simulation uses the current (overloaded) conditions and the values for the component loading level ($S_{measured,t}$) and station demand ($P_{h2,t}$) are retained. A second power flow simulation is carried out with the same conditions but with the refuelling station demand increased by a very small amount $\delta P_{h2,t}$ (e.g. 1 kW); the resulting updated value for component loading is retained. The respective differences between the component loadings and the station demand between the two power flow simulations indicates δS_t and $P_{h2,t}$ and allows the sensitivity factor to be calculated.

This article has been accepted for publication in a future issue of this journal, but has not been fully edited. Content may change prior to final publication. Citation information: DOI 10.1109/ACCESS.2021.3098161, IEEE Access

While the increased power demand $\Delta P^{+}_{h2,t+1}$ could relieve the observed overloading at the congested line/transformer, its final value will be subject to two other constraining factors. The first constraint is the rated power of the electrolyser (P^{+}_{elser}) which limits the scope to raise production:

$$\Delta P^{+}_{h2,t+1} \leq P^{+}_{elser} - P_{h2,t} \quad (17)$$

The second is the remaining available storage capacity:

$$\Delta P^{+}_{h2,t+1} \leq \frac{E^{rated}_{stor} - SOC_{\mathrm{stor},t} + H_{2\,dem,t} \cdot HHV_{h2}}{\tau_t\, \eta_{stn}} - P_{h2,t} \quad (18)$$

The maximum feasible change from Eq. (16)-(18) determines the increase in setpoint for overproduction applied in Eq. (15).

It is also important to record the accumulated 'overproduced' hydrogen ($E^{acm}_{h2,t}$) in the storage tanks at the end of each period so as to indicate the subsequent actions required to restore the SOC level back to its scheduled value:

$$E^{acm}_{h2,t+1} = E^{acm}_{h2,t} + \Delta P^{+}_{h2,t+1} \cdot \eta_{stn} \cdot \tau_t \quad (19)$$

3) UNDERPRODUCTION

The process of overproducing hydrogen means that more hydrogen is stored than was scheduled day-ahead. This amount of overcharged hydrogen would need to be released soon so that the onsite storage can return to its planned position so that the station is capable of providing support for the upcoming periods. To do so, a period of 'underproduction' will be necessary to reduce the amount of 'overstored' hydrogen by producing less than the scheduled level. The decision-making process for underproduction is triggered at the end of time step t if the accumulated overproduced hydrogen in storage has not been fully released (i.e. $E^{acm}_{stor,t} \neq 0$). The change in station power consumption for the following time step is:

$$P_{h2,t+1} = P_{h2,t} - \Delta P^{-}_{h2,t+1} \quad (20)$$

where the reduction in power consumption $\Delta P^{-}_{h2,t+1}$ necessary to return hydrogen storage level to the scheduled level is given by:

$$\Delta P^{-}_{h2,t+1} \leq \frac{E^{acm}_{h2,t}}{\tau_t\, \eta_{stn}} \quad (21)$$

In contrast to overproduction, underproduction will tend to increase the loading of the line or transformer nearby, as a result of less local electricity consumption and more DG output being exported. Reduction in production must not result in the power flow exceeding thermal limits (or more accurately, the threshold), implying a constraint on the extent of change between periods:

$$\Delta P^{-}_{h2,t+1} \leq \frac{S_{targeted} - S_{measured,t}}{\delta S_t \,/\, \delta P_{h2,t}} \quad (22)$$

where $\Delta P^{-}_{h2,t+1}$ is also estimated using a similar sequence of power flow simulations as in Section III.C.2 but this time using a *decrease* in station demand. Additionally, in some cases the minimum allowed electrolyser operational level P^{-}_{elser} may apply, limiting the extent of reduction between periods:

$$\Delta P^{-}_{h2,t+1} \leq P_{h2,t} - P^{-}_{elser} \quad (23)$$

The maximum feasible change from Eq. (21)-(23) defines the new setpoint in (20). At the end of the undercharging period $E^{acm}_{stor,t+1}$ is also updated accordingly.

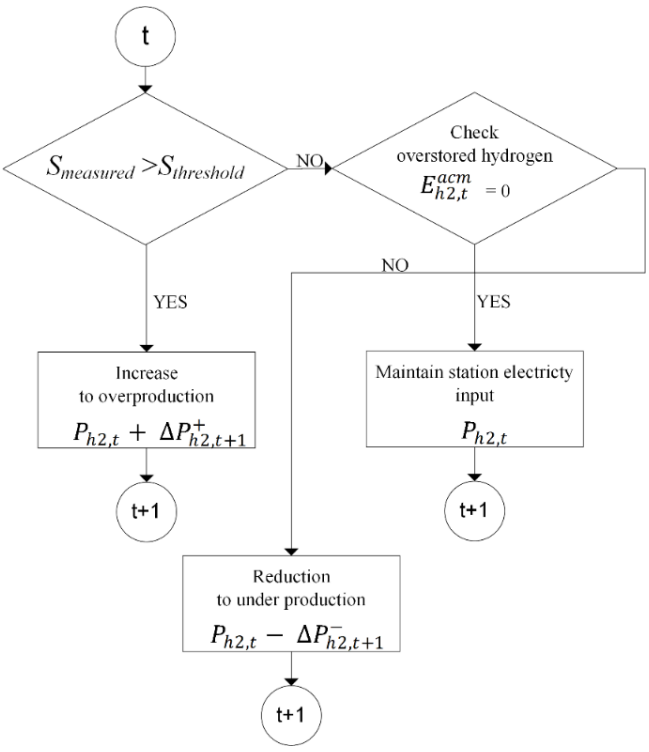

FIGURE 4. Control logic of 'active' operational approach: changes in production in response to network conditions.

IV. CASE STUDY

To demonstrate the refuelling station control strategies, a simplified five bus network representing a distribution network in a wind-rich area is studied, as shown in Figure 5. The demand and transformer data are based on a typical 11 kV network. Peak demand (excluding refuelling station demand) is 3MW and there is a 6MVA transformer connecting to the 33 kV higher voltage network.

This article has been accepted for publication in a future issue of this journal, but has not been fully edited. Content may change prior to final publication. Citation information: DOI 10.1109/ACCESS.2021.3098161, IEEE Access

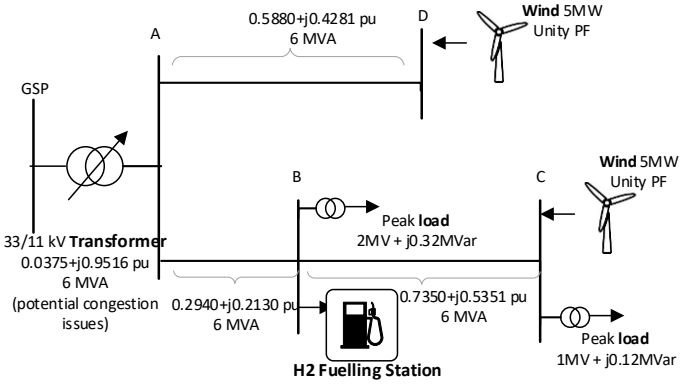

FIGURE 5. 11kV network case in wind rich area with hydrogen refuelling station connected. Network parameters (resistance, reactance and thermal capacity) and load data (peak active and reactive load) are provided alongside each component. For line impendences, their value is given as per unit (pu) on 100-MVA base.

The refuelling station's peak day hydrogen fuel demand is assumed to be 560kg, based on 100 FCEVs being refilled (5.6 kg on average). A week long profile of station hydrogen demand is shown in Figure 6. This is shown as the percentage of peak day total and is derived from a modified Chevron™ profile in the H2A analysis H2A Delivery Scenario Analysis Model Version 3.0 (HDSAM 3.0) [36]. The original profile is adjusted to represent station closure during the night.

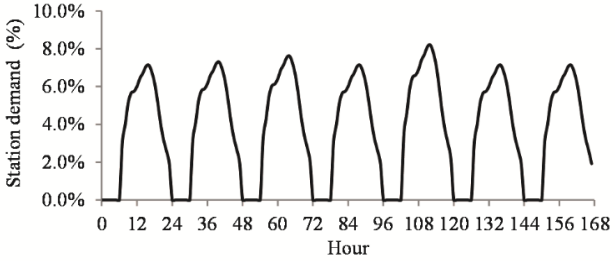

FIGURE 6. Half-hourly refuelling station hydrogen demand over a week (Monday to Sunday)

Applying the hydrogen demand profile mentioned above, the hourly refuelling demand peaks at 47.4 kg H_2 (1.86 MW) at Friday noon. To meet its peak demand, the key parameters of the refuelling station are given in Table I. Using the efficiency assumptions, the overall conversion efficiency can be calculated as 64% using Eq. (11). Electrolysers at the station correspondingly have a rated power of 2.9 MW. The onsite storage is assumed to have half a day's capacity (17.5 MWh). The compressor is sized so that its capability is enough to handle the flow rate of the electrolysers running at their full rate.

TABLE I. REFUELLING STATION COMPONENT SIZES AND EFFICIENCIES

Component	Capacity	Efficiency
Electrolyser	2900 kW	70%
Compressor	145 kW	80%
Hydrogen tank	17500 kWh	97%

There are two wind farms in the network operating at unity power factor. A 'firm' 5 MW wind farm is connected at bus D, exporting as much as it generates. A more flexibly-connected wind farm at bus C is rated at 5 MW, which is well beyond the remaining 2 MW capacity that fit-and-forget operation of the network can host. To allow this wind farm to operate above 2 MW it is necessary to curtail production during strong wind periods and at low demand levels in order to avoid network constraints. In this network, there is a single constraint that must be managed, namely the overloading of the 33/11 kV primary transformer at the grid supply point (GSP) substation. This would be identified through offline network analysis such as those carried out by the DNO prior to connection. In this network, the control scheme requires measurement of the apparent power flow through the transformer, a remote telemetry unit and a communications link to the control system sited at the refuelling station. Different networks would require a different set of measurement and control systems tailored to their specific circumstances. To illustrate the operation of the active control scheme, a conservative threshold of 95% loading on the transformer is applied above which the control system responds to return loading to a target of 95% by the next time step. This reflects a desire to minimise power flows above the rated power of the transformer caused by fluctuations in loading conditions within the control period.

Demand and wind generation data from Scotland is used in all simulations [37]. To simplify the presentation and simulation, the levels of wind and demand are normalised (per unit) against peak values. The load factor of this wind profile is 37% and the whole year variation is illustrated in Figure 7(a) with load in summer relatively lower than winter; a five-day sample window is selected to evaluate the performance of different controls, as shown in Figure 7(b).

The control schemes are evaluated at several levels. The first, at a 1-minute time step for one hour illustrates the detailed operation of the control schemes in responding to overloading. The second, for a 5-day period illustrates intra- and inter-day effects and the influence of the storage. Finally, a year-round analysis indicates some of the important economic impacts of the different operating strategies.

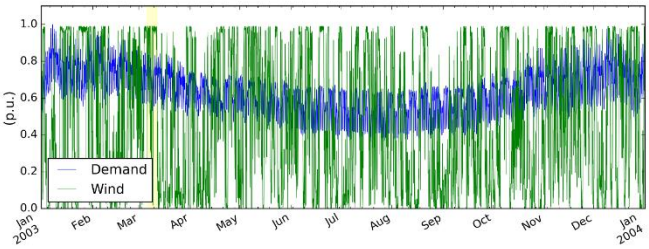

(a)

This article has been accepted for publication in a future issue of this journal, but has not been fully edited. Content may change prior to final publication. Citation information: DOI 10.1109/ACCESS.2021.3098161, IEEE Access

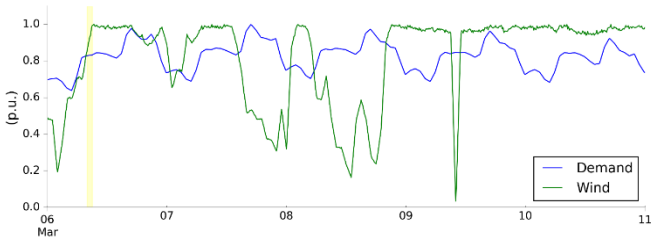

(b)

FIGURE 7. Electricity demand and wind variation: (a) for a whole year and (b) five-day sample window during winter with the 1-hour simulation period highlighted.

A. VALIDATION OF OPERATION STRATEGIES IN 1-HOUR WINDOW

The simulation of a 1 hour window at 1 minute steps is shown in detail to illustrate the impact of the active control system set out in Section III. This is contrasted with the refuelling station in steady operation mode following a scheduled, fixed 1.03 MW electricity consumption throughout the whole period. In active operation, the refuelling station is scheduled to maintain this same demand level but will diverge as required in response to the loading on the transformer.

The simulation covers a period between 08:00 and 09:00 with the variation in wind and demand shown clearly in Figure 8(a) indicating flat demand and a fluctuating but rising trend in wind output. The effects of the wind and demand patterns on the transformer loading are shown in Figure 8(b) with the steady operation trace showing loading following wind production. There are a number of instances where the loading exceeds the (100%) rating with the 95% threshold exceeded continuously from 08:50 onwards. The darker line diverges from steady operation in a number of places as the active control scheme responds to the higher loading above the threshold. Looking at the period from 08:50 the control logic can be followed. At 08:50 the electrolyser is operating at 1.03 MW (its predefined average level) and an increase in wind sees the transformer loading reach 102%. As this exceeds the 95% threshold, the sensitivity factor is calculated to determine the necessary change in station consumption. Two snapshot power flow analyses are carried out to define the change in transformer loading with a small change in station electricity consumption: the sensitivity factor is found to be 17% per MW change. This is used in (16) to calculate the necessary increase in power input for the next minute (08:51) to return loading to the 95% target:

$$\Delta P^{+}_{h2,t=8:51} = \frac{102\% - 95\%}{17\% \,/\, 1\ \mathrm{MW}} = 0.41\mathrm{MW}$$

The electrolyser rating and storage limits do not act to constrain this change. When the control action is applied, it can be seen that at 08:51 the increased station setpoint of 1.44MW ($1.03\mathrm{MW} + 0.41\mathrm{MW}$) successfully reduces the transformer loading. However, the loading is 100% as a result of wind production increasing and the steady operation case shows it would have been 107% had no action been taken by the controller; the counteracting of the control effect reinforces the case for conservative threshold levels. As loading remains above the threshold, overproduction remains activated for 08:52, with a new sensitivity factor calculated and the station setpoint increased to 1.74MW.

The actual loading at 08:52 turns out to be 93%, as a result of the wind speed reducing in this minute. This leaves 2% headroom for the station to (partly) return from overproduction. Given that the accumulated overproduced hydrogen in the tanks from the previous time periods up to 8:52 has not been fully released ($E^{acm}_{h2,t} = 0.03\mathrm{MWh}$), underproduction is activated from 08:53. The reduction required to fully release overcharged storage is calculated using (21):

$$\Delta P^{acm}_{h2,t=8:53} = \frac{-0.03\mathrm{MWh}}{1\mathrm{min} \times 0.63} = -2.8\mathrm{MW}$$

However, the reduction is subject to the available headroom at the transformer (i.e. the threshold), which after calculating a new sensitivity factor (20%/MW) is estimated as:

$$\Delta P^{-}_{h2,t=8:53} = \frac{95\% - 93\%}{20\% \,/\, 1\ \mathrm{MW}} = 0.1\mathrm{MW}$$

The refuelling station setpoint is therefore reduced to 1.64 MW for 08:53 (1.74MW – 0.1MW). Figure 8(c) shows that at 08:53, the transformer maintains below target loading. The elevated levels of wind production in this period do not allow reductions below the scheduled production level (1.03 MW) and as a result additional hydrogen accumulates in storage, as Figure 8(d) illustrates.

Overall, the active control is effective in reducing overloading with the duration reduced to 3 minutes from 13 minutes for steady operation. The control system can be 'tuned' by adjusting the time interval, threshold and target loading levels to deliver the desired balance of speed, overloading and degree of response from the refuelling station.

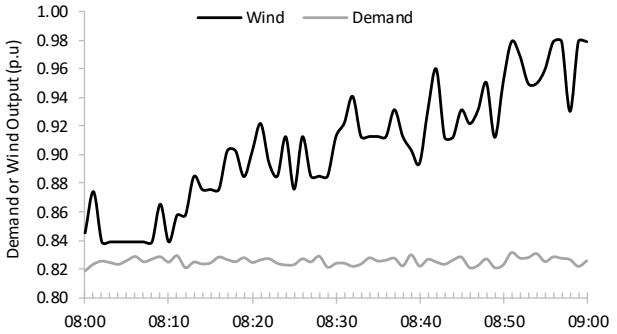

(a)

This article has been accepted for publication in a future issue of this journal, but has not been fully edited. Content may change prior to final publication. Citation information: DOI 10.1109/ACCESS.2021.3098161, IEEE Access

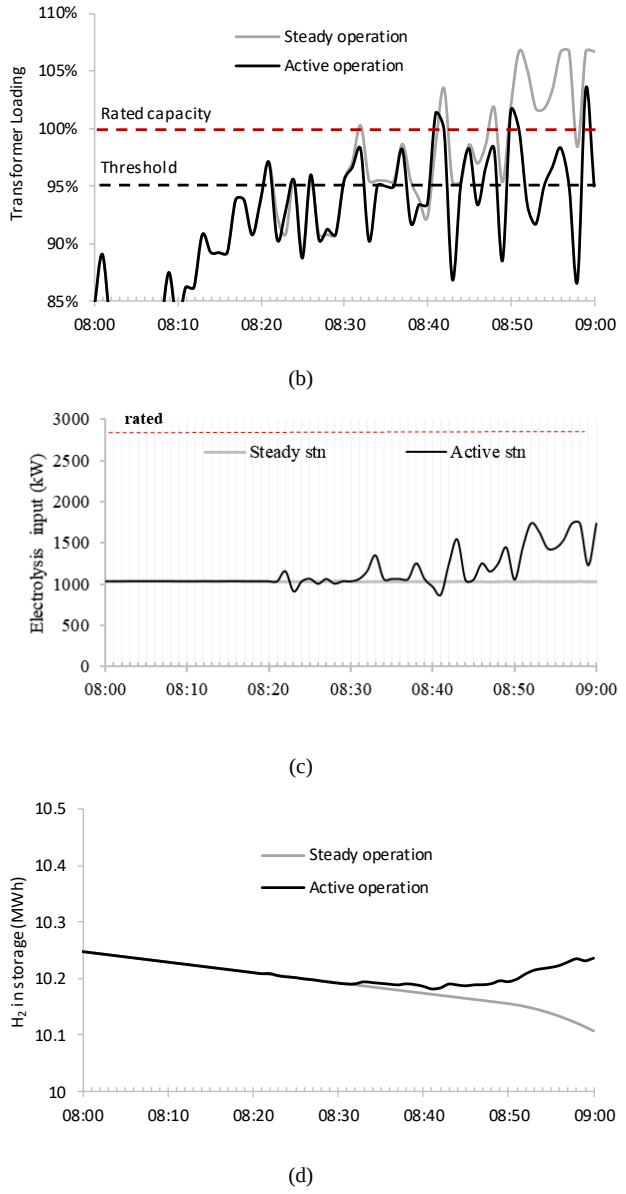

FIGURE 8. 1-min time step simulation of steady operation and active control: (a) wind and demand; (b) transformer loading; (c) station electricity demand; and (d) hydrogen in store

B. EVALUATION OF OPERATION STRATEGIES FOR 5-DAY WINDOW

To assess the performance of the operation strategy over a longer period of time, the 5-day sample window depicting network operation in winter with strong wind is studied (Figure 7(b)). The scenarios include network cases without a refuelling station and with the refuelling station in passive, steady and active operation modes. The scheduled rate of electricity consumption in the steady and active operation cases is the average of the refuelling station demand of each day.

The scenario without a refuelling station provides a benchmark for the impacts that the connection of a refuelling station may have. Figure 9(a) clearly shows a great number of overloading events due to the excess production from the wind farm and a lack of local consumption. Comparing this with the passive operation results shows that a considerable amount of overloading during the day time is avoided due to the operation of the refuelling station during this period (Figure 9(b)). The remaining thermal constraints during the night are partly mitigated in the steady operation case once the refuelling station makes use of the storage capacity in ensuring consumption throughout the day. Lastly, almost of all the overloading at the transformer is avoided when the refuelling station operates actively by increasing hydrogen production during the period when the network is constrained (Figure 9(b), and subsequently reducing its electricity consumption once the network is not constrained.

Using the active operation strategy is effective in maintaining the transformer loading below its limits even during strong wind periods. This means there is little or no need for other control schemes to manage this constraint, such as curtailment of the output of wind farm C. Curtailment in each operation strategy varies considerably: 52.9 MWh for passive operation, 21.6 MWh for steady operation and 4.1 MWh for active operation. Compared to the passive case, operating actively reduces curtailment by 92% and, under the assumption that the transformer can tolerate short term overloading (which would be normal), then the active operation refuelling station scheme can fully avoid the need for curtailment at wind farm C.

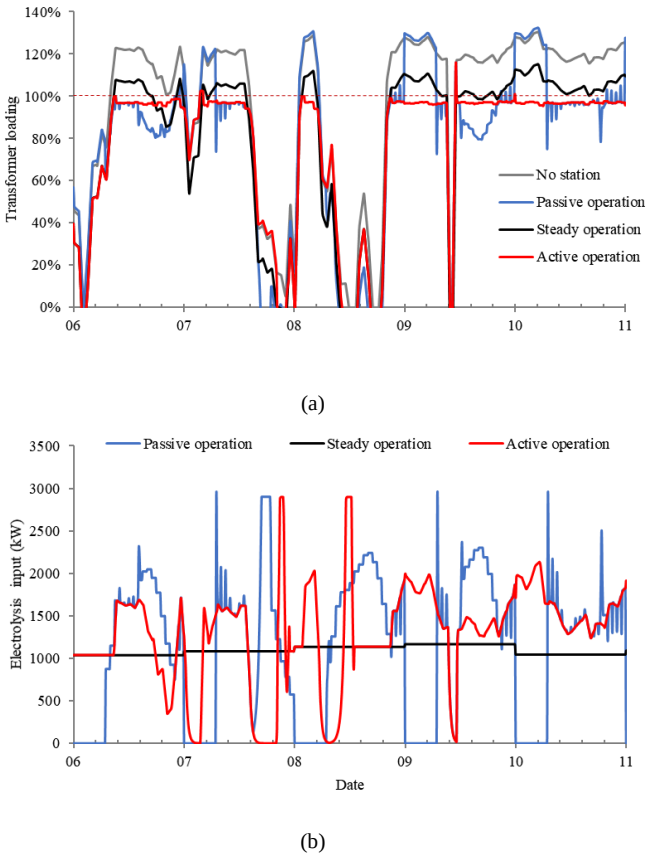

This article has been accepted for publication in a future issue of this journal, but has not been fully edited. Content may change prior to final publication. Citation information: DOI 10.1109/ACCESS.2021.3098161, IEEE Access

FIGURE 9. 5-day simulation: (a) transformer loading; (b) electrolysis input.

C. ANNUAL EVALUATION

The simulation described in the previous section was repeated for the whole year with the passive, steady and active control strategies. Where the operation of the refuelling station results in a reduction in curtailment from wind farm C, this is shown in the bar chart in Figure 10. The fact that there is additional demand means that some curtailment is avoided simply by the operation of the refuelling station coinciding with periods of peak wind production and/or low electricity demand. Active control enables wind farm C to save 5.8 GWh of otherwise curtailed electricity over the year, some 9.5 times more than the amount avoided under passive control and 5.2 times more than with steady control.

The economic impact of the different operational strategies is useful to consider as this has implications for the incentives for coupling different markets. In practice, the economic effect of the control actions will depend very much on the regulatory practices surrounding how curtailed renewable generation is compensated (or not), the effect and design of subsidies (if any) and whether there is a local market or a more straightforward arrangement between the refuelling station, wind farm and distribution company. However, a first level estimate is possible using a few fairly simple assumptions.

The operational cost of the refuelling station over the year is calculated as:

$$C_{opt} = \sum_{t} (E_{grid,t} C_{grid,t} + E_{exs,t} C_{exs}) - R_{exs} \qquad (24)$$

where E_{grid} is the electricity consumed by the refuelling station that is deemed to be supplied 'normally' from the grid at a price C_{grid} which can vary with time or be a fixed price. The energy consumed by the refuelling station that is as a result of active control to relieve network constraints, is deemed to be the avoided curtailment from the wind farm E_{exs}; this is assumed to attract a different price C_{exs} that might conceivably be at a lower price or even 'free'. The avoided curtailment under the passive and steady control is not due to actively responding to network conditions but as a byproduct of their operation; therefore, they are not attributed this 'cheap' electricity. In addition, the refuelling station may receive rewards (R_{exs}) for providing services to help relieve network constraints and so avoid or delay costly network reinforcement [38]. As a result of active control strategy, this reward is subtracted from the total operational cost.

The standard electricity price paid by the refuelling station C_{grid} is taken to be a uniform £50/MWh [39] but two different scenarios are considered regarding the treatment of the avoided curtailment and the services 'reward':

1. The electricity consumed as a result of actively avoiding curtailment C_{exs} is at zero cost and there is no explicit reward for services;
2. The electricity consumed as a result of actively avoiding curtailment C_{exs} is at zero cost but a service reward R_{exs} of £30 per MWh of avoided curtailment applied; this effectively delivers a negative price of -£30/MWh for wind farm production under constrained situations.

As can be seen from the line plot in Figure 10, under the first pricing approach the active control case has much lower yearly net cost of electricity at £3.16M, which is 7.5% cheaper than the passive and steady operation cases. For the second pricing case, a further 5% cost reduction arises.

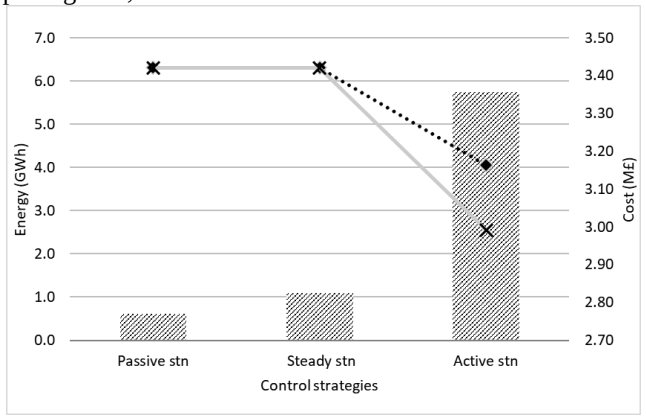

FIGURE 10. Total avoided curtailment (shaded) and the total fuel cost (with rewards (crosses) and without rewards (diamonds)) of the refuelling station at wind farm C for a whole year evaluation with different control strategies

D. IMPACT OF FORECAST AND OTHER ERRORS

There are several potential sources of error in the approach used in this analysis relating to the effects of the sensitivity factor method and persistence forecasting.

Linearization using the sensitivity factor approach does result in the realised transformer loading level at each point of time being slightly different to that which would have been achieved using a fully nonlinear approach. There are two aspects to this: (1) that only a single location is considered in terms of being monitored for overloading and (2) that linearization will result in some error relative to the true nonlinear state. The method focuses purely on the critical component loading as this the only constraint we are 'measuring' and as long as this is managed there are no other network violations. As such, the impact of a lack of visibility of rest of the network state is minimal; in more complex situations this might be a significant issue. Linearization does have an impact but over the range of analyses conducted the maximum error between the target component loading and the realised loading was equivalent to 0.18% of the transformer rating. Overall, the errors due to the sensitivity factor approach are modest.

The proposed control strategy employs a persistence forecasting approach in the absence of wind and demand forecasts at the sites, wherein the calculation assumes the demand and wind production at time $t+1$ will be the same the same as t. This implies that the control action is only triggered after the violation of a threshold occurs, and the targets are unlikely to be precisely achieved. To investigate the effect of

This article has been accepted for publication in a future issue of this journal, but has not been fully edited. Content may change prior to final publication. Citation information: DOI 10.1109/ACCESS.2021.3098161, IEEE Access

forecast error, the case in Section IV.A was repeated with control under perfect foresight with future values known. The comparative results are provided in Figure 11. Compared with the persistence forecast based control, control using perfect foresight results in earlier action to change station electricity input consumption (Figure 11.b). This has the effect of maintaining the transformer loading below the target threshold value (95% of the transformer rating) at all times (Figure 11.a). It can be concluded that with perfect forecasts, a preventive effect is brought into the constraint management. Moreover, the perfect forecast would enable a reduction in the safety margin allowing the raising of the trigger threshold closer to the full transformer rating and so allow more local renewable being exported.

In practice, however, a perfect forecast is impossible. As demonstrated in the previous sections, by properly choosing a threshold, the persistence forecast based control strategy is able to achieve effective overloading management in real time with very few violations. In addition, the control running at short time steps will tend to further limit the duration of these violations. The persistence forecast-based control shows that a minimum but acceptable performance level can be achieved.

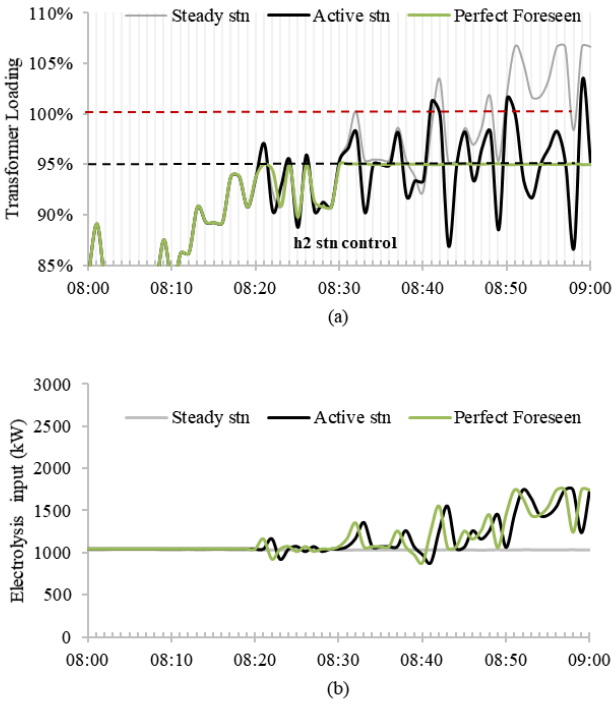

FIGURE 11. Comparison of transformer loading (a) and H2 Station electrolysis inputs (b) under three different control scenarios: steady (passive) mode, active control mode with persistence forecasting and active control with perfect forecasting

V. DISCUSSION

The case study demonstrates that active operation of hydrogen refuelling stations can help manage the overloading issues caused by high DG production. Over the study period, the active control of the refuelling station supports renewable integration through considerable avoided curtailment, and potentially reducing the station's operational cost. Therefore, the effectiveness of the proposed active operation strategy of hydrogen refuelling stations to bring benefits for the whole integrated local system is validated. The paper uses a sensitivity factor method for active network management to illustrate the value of operating hydrogen refuelling stations in an active manner. The proposed control strategy employs a persistence forecasting approach which means control targets are unlikely to be precisely achieved. However, with the control running at short time steps and careful choice of thresholds will tend to limit these errors. Further improvements of the control scheme would include short-term forecasting to limit overloading events and allow safety margin to be reduced.

This sensitivity factor approach needs a small number of measurements at the likely congestion point and the refuelling station as well as communications links. There are a number of possible ways of implementing this approach in practice: (i) using a lookup table with sensitivities calculated offline, (ii) a digital twin of the network where the above algorithm is implemented, or (iii) a form of real time online perturbation of demand with the change in power flow giving the sensitivity. However, it should be stressed that other active network approaches in the literature could make use of the general modelling approach to examine the integration of hydrogen refuelling stations.

A wind-rich distribution network is investigated in the case study. It is a simplified network but clearly captures the coordination required between the network constraint and the point of connection of the refuelling station. The conclusion is general, and the active control is applicable to other networks that are stressed by high PV, small-hydro generation or their combinations. For different networks and renewables, the occurrences of periods of network constraints may be different [37] and so will the need for support from the hydrogen station. The control setting and the economic performance can be analysed using the proposed model on a case-by-case basis. Equally, the general approach could be applied to networks that have constraints arising from high peak demand, where more active control of the refuelling station to avoid station operation at peak load could avoid or defer network reinforcement.

The model of the station is a simple linear model with fixed efficiency and as such does not account for nonlinear or dynamic effects. In reality the characteristics of PEM stations mean the variation in efficiency is more complex but falls by around 5 percentage points over a large operating range (25 – 100% of rated) [40]. A full analysis of the importance of this simplification would require a new and fully realistic efficiency curve within the model. However, a first level comparison of the operating modes can be gained by cross-referencing the efficiency that would apply at each level of station output. Analysis of the 5-day simulation (Section IV.B)

This article has been accepted for publication in a future issue of this journal, but has not been fully edited. Content may change prior to final publication. Citation information: DOI 10.1109/ACCESS.2021.3098161, IEEE Access

showed that steady operation was most efficient, with passive and then active control around 2% lower, largely due to operation at higher as well as much lower production levels. That period, however, was particularly windy and variable so it is postulated that the efficiency 'loss' associated with active control would be more modest over a longer period; further work would establish this. Capturing the impact of dynamic changes on efficiency would require a much more sophisticated dynamic model, although the literature suggests that PEM stations [40] are relatively insensitive to rapid variations in output. Analysis of the inter-period ramping during the 5-day simulation showed that the passive case had considerable variations in production, some of which as large as 10%/min. Active operation saw around 50% more ramps but these tended to be smaller (max 4%/min). More detailed analysis of this effect would be valuable future work.

In the case study, the rated power of the electrolyser is sized to meet the peak demand of the refuelling, as required by the passive operational strategy. While it helps set the comparison of the strategies on the same basis, it is oversized for the steady and active control strategies, which normally only make use of around half of its capacity, except when responding to network management requirements. Therefore, it leaves considerable headroom for active control to adjust the station load. Reducing the capacity of the electrolyser will reduce the capital cost, but at the expense of decreased capability to relieve network constraints and would offer less opportunity to generate hydrogen from constrained renewables. This trade-off effect clearly forms a further research question around optimal sizing of the station to minimise overall capital and operating costs for specific control strategies.

An analytical approach is adapted in this study to look at the performance of the hydrogen refuelling station. Simulation is performed at minute-by-minute steps. To achieve better coherence between planning decision and operational strategies, an integrated techno-economic model that optimises the size of the station components, with detailed modelling of control and distribution network AC power flow, is desirable. In terms of mathematical programming, such a model would be mixed-integer (due to the charging/discharging behaviour and directed control), non-linear (due the AC power flow, strong non-convex), dynamic programming class. It is very challenging to solve [41], [42] and an area of future research.

There are other designs of electrically-powered hydrogen refuelling stations. For example, it may have its own on-site power generation system, which comprises a stand-alone system that can be implemented at locations where connections to electricity grids are not easily accessible [43], [44]. In this study, analysis considers networks with already existing high penetrations of renewable generation that stress the network; the implementation of active control to provide ancillary service of flexibility to the network operator and renewable developers has demonstrated considerable benefits. In this way, hydrogen refuelling stations could potentially benefit the distribution company and renewable developers, rather than just impose challenges.

VI. CONCLUSION

Power-to-hydrogen conversion at FCEV refuelling stations creates an interlinked local energy system between the electricity, hydrogen and transportation sectors. Here, an active control scheme has been presented wherein the electricity consumption of the refuelling station is adaptively changed to manage the network constraints in networks with high renewable generation. As validated by the case study, the active control of the refuelling station supports renewable integration with considerable avoided curtailment, potentially reducing the station's operational cost over the study period. The work provides enhanced understanding of the impact of deploying hydrogen refuelling stations and motivating relevant stakeholders to explore its full value, especially by means of coupling electricity, hydrogen and transportation to provide flexibility to handle renewable variability and avoid electricity network reinforcement. In future study, further improvements of the control scheme could include short-term forecasting and consider its adaption with limited visibility of network.

REFERENCES

[1] J. Delbeke, *EU Climate Policy Explained*. Routledge, 2015.
[2] IPCC, "Climate change 2014: mitigation of climate change." Cambridge University Press, 2015.
[3] F. Creutzig *et al.*, "Transport: A roadblock to climate change mitigation?," *Science*, vol. 350, no. 6263, pp. 911–912, 2015.
[4] I. Staffell *et al.*, "The role of hydrogen and fuel cells in the global energy system," *Energy & Environmental Science*, vol. 12, no. 2, pp. 463–491, Feb. 2019.
[5] S. Pique, B. Weinberger, V. De-Dianous, and B. Debray, "Comparative study of regulations, codes and standards and practices on hydrogen fuelling stations," *International Journal of Hydrogen Energy*, vol. 42, no. 11, pp. 7429–7439, Mar. 2017.
[6] J. Howes, "Hydrogen and Fuel Cells: Opportunities for Growth A Roadmap for the UK E4tech and Element Energy," 2016.
[7] P. E. Dodds and S. Demoullin, "Conversion of the UK gas system to transport hydrogen," *International Journal of Hydrogen Energy*, vol. 38, no. 18, pp. 7189–7200, Jun. 2013.
[8] M. Z. Jacobson, W. G. Colella, and D. M. Golden, "Atmospheric science: Cleaning the air and improving health with hydrogen fuel-cell vehicles," *Science*, vol. 308, no. 5730, pp. 1901–1905, Jun. 2005.
[9] H. Xu, I. Kockar, S. Schnittger, and J. Rose, "Influences of a hydrogen electrolyser demand on distribution network under different operational constraints and electricity pricing scenarios," in *CIRED Workshop -Helsinki*, 2016.
[10] R. M. Oviedo, Z. Fan, and M. Sooriyabandara, "Ecoisland: A hydrogen refueler and storage system with renewable energy sources," in *2014 IEEE PES T&D Conference and Exposition*, 2014, pp. 1–5.
[11] A. A. Akhil *et al.*, "DOE/EPRI Electricity Storage Handbook in Collaboration with NRECA," United States, 2015.
[12] E. Rothuizen and M. Rokni, "Optimization of the overall energy consumption in cascade fueling stations for hydrogen vehicles," *International Journal of Hydrogen Energy*, vol. 39, no. 1, pp. 582–592, 2014.
[13] E. Rothuizen, W. Mérida, M. Rokni, and M. Wistoft-Ibsen, "Optimization of hydrogen vehicle refueling via dynamic simulation," *International Journal of Hydrogen Energy*, vol. 38, no. 11, pp. 4221–4231, 2013.
[14] H. Dagdougui, A. Ouammi, and R. Sacile, "Modelling and

control of hydrogen and energy flows in a network of green hydrogen refuelling stations powered by mixed renewable energy systems," *International Journal of Hydrogen Energy*, vol. 37, no. 6, pp. 5360–5371, 2012.

[15] M. Kiaee, A. Cruden, D. Infield, and P. Chladek, "Utilisation of alkaline electrolysers to improve power system frequency stability with a high penetration of wind power," *Iet Renewable Power Generation*, vol. 8, no. 5, pp. 529–536, 2014.

[16] S. Carr, G. C. Premier, A. J. Guwy, R. M. Dinsdale, and J. Maddy, "Hydrogen storage and demand to increase wind power onto electricity distribution networks," *International Journal of Hydrogen Energy*, vol. 39, no. 19, pp. 10195–10207, 2014.

[17] S. Carr, F. Zhang, F. Liu, Z. L. Du, and J. Maddy, "Optimal operation of a hydrogen refuelling station combined with wind power in the electricity market," *International Journal of Hydrogen Energy*, vol. 41, no. 46, pp. 21057–21066, 2016.

[18] G. Andersson and G. Hug-Glanzmann, "Bacterial foraging optimisation: Nelder–Mead hybrid algorithm for economic load dispatch," *IET Generation, Transmission & Distribution*, vol. 1, no. September 2007, pp. 492–498, 2008.

[19] T. Sansawatt, L. F. Ochoa, and G. P. Harrison, "Smart Decentralized Control of DG for Voltage and Thermal Constraint Management," *IEEE Transactions on Power Systems*, vol. 27, no. 3, pp. 1637–1645, Aug. 2012.

[20] J. G. Robertson, G. P. Harrison, and A. R. Wallace, "OPF Techniques for Real-Time Active Management of Distribution Networks," *IEEE Transactions on Power Systems*, vol. 32, no. 5, pp. 3529–3537, Sep. 2017.

[21] J. Quirós-Tortós, L. F. Ochoa, S. W. Alnaser, and T. Butler, "Control of EV Charging Points for Thermal and Voltage Management of LV Networks," *IEEE Transactions on Power Systems*, vol. 31, no. 4, pp. 3028–3039, 2016.

[22] W. Sun and G. Harrison, "Active operation of hydrogen fuelling stations to support renewable integration," *2017 IEEE PES Innovative Smart Grid Technologies Conference Europe, ISGT-Europe 2017 - Proceedings*, vol. 2018-Janua, pp. 1–6, 2018.

[23] I. Staffell *et al.*, "The role of hydrogen and fuel cells in the global energy system," *Energy and Environmental Science*, vol. 12, no. 2. Royal Society of Chemistry, pp. 463–491, 01-Feb-2019.

[24] M. Z. Jacobson, M. A. Delucchi, M. A. Cameron, and B. V. Mathiesen, "Matching demand with supply at low cost in 139 countries among 20 world regions with 100% intermittent wind, water, and sunlight (WWS) for all purposes," *Renewable Energy*, vol. 123, pp. 236–248, Aug. 2018.

[25] M. Z. Jacobson *et al.*, "Impacts of Green New Deal Energy Plans on Grid Stability, Costs, Jobs, Health, and Climate in 143 Countries," *One Earth*, vol. 1, no. 4, pp. 449–463, Dec. 2019.

[26] F. Grüger, L. Dylewski, M. Robinius, and D. Stolten, "Carsharing with fuel cell vehicles: Sizing hydrogen refueling stations based on refueling behavior," *Applied Energy*, vol. 228, pp. 1540–1549, Oct. 2018.

[27] H. Fayaz, R. Saidur, N. Razali, F. S. Anuar, A. R. Saleman, and M. R. Islam, "An overview of hydrogen as a vehicle fuel," *Renewable and Sustainable Energy Reviews*, vol. 16, no. 8, pp. 5511–5528, Oct. 2012.

[28] M. Thema, F. Bauer, and M. Sterner, "Power-to-Gas: Electrolysis and methanation status review," *Renewable and Sustainable Energy Reviews*, vol. 112, pp. 775–787, Sep. 2019.

[29] M. Carmo, D. L. Fritz, J. Mergel, and D. Stolten, "A comprehensive review on PEM water electrolysis," *International Journal of Hydrogen Energy*, vol. 38, no. 12, pp. 4901–4934, Apr. 2013.

[30] M. David, C. Ocampo-Martínez, and R. Sánchez-Peña, "Advances in alkaline water electrolyzers: A review," *Journal of Energy Storage*, vol. 23, pp. 392–403, Jun. 2019.

[31] A. Mayyas and M. Mann, "Manufacturing competitiveness analysis for hydrogen refueling stations," *International Journal of Hydrogen Energy*, vol. 44, no. 18, pp. 9121–9142, Apr. 2019.

[32] C.-H. Li, X.-J. Zhu, G.-Y. Cao, S. Sui, and M.-R. Hu, "Dynamic modeling and sizing optimization of stand-alone photovoltaic power systems using hybrid energy storage technology," *Renewable Energy*, vol. 34, no. 3, pp. 815–826, Mar. 2009.

[33] S. Nistor, S. Dave, Z. Fan, and M. Sooriyabandara, "Technical and economic analysis of hydrogen refuelling," *Applied Energy*, vol. 167, pp. 211–220, Apr. 2016.

[34] R. C. Dugan, "The Open Distribution System Simulator (OpenDSS)," *Electric Power Research Institute, Inc.*, no. November, pp. 1–177, 2012.

[35] S. C. E. Jupe, P. C. Taylor, and A. Michiorri, "Coordinated output control of multiple distributed generation schemes," *IET Renewable Power Generation*, vol. 4, no. 3, p. 283, 2010.

[36] Argonne National Laboratory: Centre for Transportation Research, "H2A Delivery Scenario Analysis Model Version 3.0 (HDSAM 3.0) User's Manual. ," 2015.

[37] W. Sun and G. P. Harrison, "Wind-solar complementarity and effective use of distribution network capacity," *Applied Energy*, vol. 247, pp. 89–101, Aug. 2019.

[38] D. T. C. Wang, L. F. Ochoa, and G. P. Harrison, "DG impact on investment deferral: Network planning and security of supply," *IEEE Transactions on Power Systems*, vol. 25, no. 2, pp. 1134–1141, 2010.

[39] Office of Gas and Electricity Markets (Ofgem), "State of the energy market 2018," 2018.

[40] A. Buttler and H. Spliethoff, "Current status of water electrolysis for energy storage, grid balancing and sector coupling via power-to-gas and power-to-liquids: A review," *Renewable and Sustainable Energy Reviews*, vol. 82, pp. 2440–2454, Feb. 2018.

[41] W. A. Bukhsh, A. Grothey, K. I. M. M. McKinnon, and P. A. Trodden, "Local solutions of the optimal power flow problem," *IEEE Transactions on Power Systems*, vol. 28, no. 4, pp. 4780–4788, Nov. 2013.

[42] B. Kocuk, S. S. Dey, and X. A. Sun, "Strong SOCP Relaxations for the Optimal Power Flow Problem," no. Carpentier 1962, pp. 1–40, 2015.

[43] M. Gökçek and C. Kale, "Techno-economical evaluation of a hydrogen refuelling station powered by Wind-PV hybrid power system: A case study for İzmir-Çeşme," *International Journal of Hydrogen Energy*, vol. 43, no. 23, pp. 10615–10625, Jun. 2018.

[44] S. H. Siyal, D. Mentis, and M. Howells, "Economic analysis of standalone wind-powered hydrogen refueling stations for road transport at selected sites in Sweden," *International Journal of Hydrogen Energy*, vol. 40, no. 32, pp. 9855–9865, Aug. 2015.

Wei Sun (S'11, M'15) received the Ph.D. degree in power system engineering from the University of Edinburgh, U.K., where he is currently a Research Associate on multi-vector energy system.

Dr. Sun's research interest is in the development and application of optimization methods to the planning, design and operation of smart energy systems. He is currently working on building a multi-scale energy system integration architecture for National Centre for Energy Systems Integration (CESI) and previously as a lead researcher on Hydrogen's Value in the Energy system (HYVE). He has also contributed to EPSRC funded projects including Realising Energy Storage Technologies in Low-carbon Energy Systems (RESTLESS) and Adaptation and Resilience In Energy Systems (ARIES).

This article has been accepted for publication in a future issue of this journal, but has not been fully edited. Content may change prior to final publication. Citation information: DOI 10.1109/ACCESS.2021.3098161, IEEE Access

Gareth P. Harrison (M'02, SM'14) is Bert Whittington Chair of Electrical Power Engineering and Deputy Head of the School of Engineering at the University of Edinburgh. He holds a Bachelor's degree and a Doctorate from the same institution.

Professor Harrison leads research activity across a wide area including integration of renewable energy within multi-vector energy systems, renewable resource assessment, climate change impacts on energy systems; and carbon footprints of energy systems. He is Associate Director of the National Centre for Energy Systems Integration (CESI), was previously Principal Investigator of the Adaptation and Resilience in Energy Systems project and is currently a Co-investigator on a range of EPSRC and EU projects covering energy storage, hydrogen, conventional generation and offshore renewable energy.

Professor Harrison is a Chartered Engineer, a Fellow of the IET, a Senior Member of the IEEE and an Affiliate of the ACCA.